



## Synchronous precipitation reduction in the American Tropics associated with Heinrich 2

Martín Medina-Elizalde, Stephen J. Burns, Josué Polanco-Martinez, Fernanda Lases-Hernández, Raymond Bradley, Hao-Cheng Wang, Chuan-Chou Shen

### ► To cite this version:

Martín Medina-Elizalde, Stephen J. Burns, Josué Polanco-Martinez, Fernanda Lases-Hernández, Raymond Bradley, et al.. Synchronous precipitation reduction in the American Tropics associated with Heinrich 2. Scientific Reports, 2017, 7, 10.1038/s41598-017-11742-8 . insu-03678723

**HAL Id: insu-03678723**

**<https://insu.hal.science/insu-03678723>**

Submitted on 25 May 2022

**HAL** is a multi-disciplinary open access archive for the deposit and dissemination of scientific research documents, whether they are published or not. The documents may come from teaching and research institutions in France or abroad, or from public or private research centers.

L'archive ouverte pluridisciplinaire **HAL**, est destinée au dépôt et à la diffusion de documents scientifiques de niveau recherche, publiés ou non, émanant des établissements d'enseignement et de recherche français ou étrangers, des laboratoires publics ou privés.



Distributed under a Creative Commons Attribution 4.0 International License

# SCIENTIFIC REPORTS

OPEN

## Synchronous precipitation reduction in the American Tropics associated with Heinrich 2

Martín Medina-Elizalde<sup>1</sup>, Stephen J. Burns<sup>2</sup>, Josué Polanco-Martínez<sup>3,4,5</sup>, Fernanda Lases-Hernández<sup>6</sup>, Raymond Bradley<sup>2</sup>, Hao-Cheng Wang<sup>7</sup> & Chuan-Chou Shen<sup>7</sup>

During the last ice age temperature in the North Atlantic oscillated in cycles known as Dansgaard-Oeschger (D-O) events. The magnitude of Caribbean hydroclimate change associated with D-O variability and particularly with stadial intervals, remains poorly constrained by paleoclimate records. We present a 3.3 thousand-year long stalagmite  $\delta^{18}\text{O}$  record from the Yucatan Peninsula (YP) that spans the interval between 26.5 and 23.2 thousand years before present. We estimate quantitative precipitation variability and the high resolution and dating accuracy of this record allow us to investigate how rainfall in the region responds to D-O events. Quantitative precipitation estimates are based on observed regional amount effect variability, last glacial paleotemperature records, and estimates of the last glacial oxygen isotopic composition of precipitation based on global circulation models (GCMs). The new precipitation record suggests significant low latitude hydrological responses to internal modes of climate variability and supports a role of Caribbean hydroclimate in helping Atlantic Meridional Overturning Circulation recovery during D-O events. Significant in-phase precipitation reduction across the equator in the tropical American Americas associated with Heinrich event 2 is suggested by available speleothem oxygen isotope records.

During the last ice age climate in the North Atlantic oscillated on millennial time scales from cold (stadial) to warm (interstadial) episodes, often referred to as Dansgaard-Oeschger (D-O) events<sup>1,2</sup>. These D-O events were first identified in Greenland ice cores but are expressed in terrestrial lakes, speleothems, and marine sediments from the North Atlantic, South America, Pacific and Indian Oceans<sup>3–8</sup>. The leading hypothesis to explain millennial-scale climate cycles invokes changes in the Atlantic Meridional Overturning Circulation (AMOC)<sup>9</sup>. At times, during the last glacial, the Northern Hemisphere ice sheets supplied sufficient freshwater to the North Atlantic to reduce AMOC by lowering surface ocean density<sup>10</sup>. In turn, AMOC slowdown decreased heat transport from low to high latitudes leading to cooling across the North Atlantic<sup>9</sup>. Meltwater pulses are reflected by episodes of thick ice rafted debris (IRD) deposits in the North Atlantic known as Heinrich (H) events that were generally associated with stadial episodes<sup>11–13</sup>.

There is increasing evidence that D-O cycles were associated with rapid and significant hydrological responses in tropical and subtropical regions worldwide, probably linked to the position of the Intertropical Convergence Zone (ITCZ) and its belt of convective activity. Paleoclimate records, particularly, suggest hydrological variability that is out-of-phase across the equator in the Atlantic and eastern Pacific regions on millennial time scales<sup>7,8,14,15</sup> consistent with model results of AMOC slowdown<sup>16,17</sup>. AMOC slowdown via freshwater forcing creates a thermal asymmetry across the equator that leads to a southward displacement of the ITCZ in the Atlantic and Pacific, which then enhances precipitation in South America and the opposite in North America and northern South America, such as the Cariaco Basin<sup>8,16–19</sup>. Model results suggest, furthermore, that AMOC slowdown can induce intense precipitation reductions in the North Atlantic and India of up to 80%<sup>16</sup>. The frequency and magnitude of tropical hydroclimate variability during times of AMOC reduction remain, however, largely unconstrained

<sup>1</sup>Department of Geosciences, Auburn University, Alabama, USA. <sup>2</sup>Department of Geosciences, University of Massachusetts, Amherst, MA, USA. <sup>3</sup>Basque Centre for Climate Change (BC3), Leioa, Bizkaia, Spain. <sup>4</sup>UMR CNRS 5805 EPOC, University of Bordeaux, 33615, Pessac, France. <sup>5</sup>Laboratoire Paleoclimatologie et Paléoenvironnements Marins, EPHE, PSL Research University, Pessac, France. <sup>6</sup>Department of Earth Sciences, National Autonomous University of Mexico (UNAM), D.F., Mexico. <sup>7</sup>High-Precision Mass Spectrometry and Environment Change Laboratory (HISPEC), Department of Geosciences, National Taiwan University, Taipei, Taiwan, ROC. Correspondence and requests for materials should be addressed to M.M.-E. (email: [martin.medina@auburn.edu](mailto:martin.medina@auburn.edu))

by paleoclimate records. We present a last glacial stalagmite  $\delta^{18}\text{O}$  record of Caribbean climate from the Yucatan Peninsula (YP), Mexico, and attempt to reconstruct quantitative precipitation variability to establish how rainfall in the region responds to D-O events and particularly during stadial intervals. Our precipitation estimates are based on an assessment of last glacial tropical temperatures<sup>31</sup>, shifts in the  $\delta^{18}\text{O}$  composition of precipitation suggested by global circulation models (GCMs), the observed regional amount effect<sup>23</sup>, and the assumption that temperature dependence fractionation during calcite precipitation was according to the model by Tremaine *et al.*<sup>32</sup> (more details in Methods). We acknowledge that this is a first attempt to estimate last glacial precipitation changes quantitatively and that uncertainties still remain, particularly, concerning the magnitude of the amount effect and the  $\delta^{18}\text{O}$  composition of precipitation, and biases due to potential calcite isotopic disequilibrium conditions, during this time interval. The new precipitation record spans the time between 26.4 and 23.2 ka BP, corresponding to stadial 2 (S2) in the North Greenland Ice Core Project (NGRIP)  $\delta^{18}\text{O}$  record<sup>20</sup> and covers the full duration of Heinrich event 2 (H2).

## Results and Discussion

In 2012, we retrieved a 87-cm long stalagmite specimen, named Itzamna (after the Maya god of creation), from Río Secreto Natural Reserve, a spectacular semi-inundated cave system located in Playa del Carmen City, in the Caribbean coast of the YP (20°35.244'N; 87°08.042'W) (Supplementary Fig. S1). The YP, located between the latitudes 18 and 21°N, experiences a very distinctive monsoonal precipitation cycle with up to 80% of annual precipitation falling between June and October<sup>21</sup> (Fig. S2). The dominant moisture source of the YP is the Caribbean Sea<sup>22,23</sup> and interannual precipitation in this broad region is significantly correlated with precipitation in the YP (Fig. 1).

The Itzamna stalagmite time scale for the oldest section was determined with 7 absolute U-Th dates, following methods by<sup>24–26</sup> and based on Montecarlo simulations using the COPRA software<sup>27</sup> (Table S2; Methods). This stalagmite first deposited from 26.5 ka BP to 23.2 ka BP. After a long interruption, it resumed growth at BCE 1037 and stopped growing at CE 398. The younger portion of the stalagmite that spans the interval from the Middle Preclassic Period to the Early Classic Period of Maya history (BCE 1000 to CE 400) has been published previously<sup>23</sup>. This study focuses on the stalagmite's oldest section.

The Itzamna  $\delta^{18}\text{O}$  record ( $n = 647$  isotopic analyses at 0.5 mm sampling resolution) has a resolution of  $3 \pm 1$  years (1 SD) during the time interval between 26.5 and 24.6 ka BP and of  $16 \pm 6.7$  years (1 SD) between 24.6 and 23.2 ka BP (Fig. 2B). Calcite  $\delta^{18}\text{O}$  analyses are reported relative to V-PDB and reproducibility of the standard materials is better than 0.1‰ (more details in Methods). The stalagmite  $\delta^{18}\text{O}$  record from 26.5 to ~24.5 ka BP shows no trend. At ~24.5 ka stalagmite  $\delta^{18}\text{O}$  values become progressively more positive with a statistically significant slope of  $-1.7\text{‰ kyr}^{-1}$  ( $R^2 = 0.5$ ,  $p < 0.01$ ). This positive  $\delta^{18}\text{O}$  trend is associated with a decrease in stalagmite growth rates (Fig. S3). Across the length of the record there are six significant positive  $\delta^{18}\text{O}$  shifts (2 SD from the record's mean) of relatively short duration, 1–2 decades (Fig. 2, positive shifts indicated with numbers). The three most recent shifts are associated with a positive trend that culminates in the most positive short term shift in stalagmite  $\delta^{18}\text{O}$  at 23.24 ka BP, preceding the growth hiatus mentioned above (Fig. 2).

The characteristics and physical conditions of the Río Secreto cave system monitored from the year 2014–2016 (relative humidity ~100%, stable temperature and dripwater  $\delta^{18}\text{O}$  composition), a Hendy test (Fig. S4) and isotopic equilibrium calculations (e.g. based on dripwater  $\delta^{18}\text{O}$  and temperature and fresh calcite)<sup>28</sup> suggest that Itzamna's calcite was precipitated under or near isotopic equilibrium conditions and faithfully records precipitation  $\delta^{18}\text{O}$  variability<sup>23</sup> (see Methods for more details). Precipitation  $\delta^{18}\text{O}$  in tropical regions reflects an amount effect on interannual<sup>22</sup> and seasonal timescales<sup>29</sup>, as confirmed by our instrumental data for the YP (2014–2016)<sup>23</sup>.

We estimate precipitation percent changes relative to modern precipitation amount conditions following previous protocols<sup>30</sup>. Briefly, to estimate precipitation changes, we shift the annual precipitation cycle in Playa del Carmen (5-year monthly averages, 1998–2003) and thus precipitation  $\delta^{18}\text{O}$  using the local amount effect, so that the annual amount-weighted  $\delta^{18}\text{O}$  of precipitation varies in accordance with Itzamna  $\delta^{18}\text{O}$  anomalies<sup>23,30</sup> (Fig. 2 and Table S3). Itzamna  $\delta^{18}\text{O}$  anomalies are calculated relative to the expected equilibrium  $\delta^{18}\text{O}$  composition of calcite associated with the annual precipitation amount cycle in Playa del Carmen today (1465 mm/year), after adjusting precipitation  $\delta^{18}\text{O}$  and dripwater temperatures to reflect last glacial conditions (see Methods). The full range of stalagmite  $\delta^{18}\text{O}$ -derived precipitation values are represented by combinations of estimates of last glacial regional surface temperature (from 18 °C to 20 °C)<sup>31</sup> and modern instrumentally-determined amount effect slopes ( $\delta P/\Delta P = -0.0106\text{‰/mm}$  and  $-0.0168\text{‰/mm}$ ) (see Methods; Fig. 2C).

The Itzamna  $\delta^{18}\text{O}$  record suggests that precipitation in the northeastern YP during S2 varied typically between +150% and –10% ( $72 \pm 80\%$ , 2 SD) relative to today (i.e. 1465 mm/year) similar to the regional interannual precipitation range observed today but exceeding the modern upper boundary suggested by the longest continuous instrumental record of precipitation (Kantunilkin Town, 1950–2011, +92% to –51%)<sup>23</sup> (Fig. 2C and Table S3). Based on average precipitation estimates, during the three most recent time intervals of extreme precipitation reduction, between 23.3–23.7 ka BP and centered at 24.1 and 25 ka BP, annual mean precipitation was reduced to a minimum of 395–980 mm (Fig. 2). This annual precipitation amount range can be found occurring today in the northern YP<sup>21</sup> (Fig. S5). Notably, the intense precipitation reductions between 23.2–23.7 ka BP and centered at 25 ka BP, coincide with two peak IRD depositional phases associated with H2 centered at 25 and 23.5 ka BP<sup>13</sup> (Fig. 2 horizontal gray bars).

The Itzamna  $\delta^{18}\text{O}$ -precipitation record shows significant variability on interannual and multidecadal time scales. Particularly, wavelet spectral power analysis indicates significant variability centered at periods of ~8, ~16, ~32, ~64 and ~128 years, over the first 2 kyrs of the record (Fig. 2A). We find that chronological uncertainties have little effect on these results (see Methods for more details). The record shows variability only at the higher periods from 64 to 128 years after 24.5 ka because stalagmite growth rate reduction at this time causes insufficient resolution to detect higher frequency  $\delta^{18}\text{O}$  variability (Fig. S6).

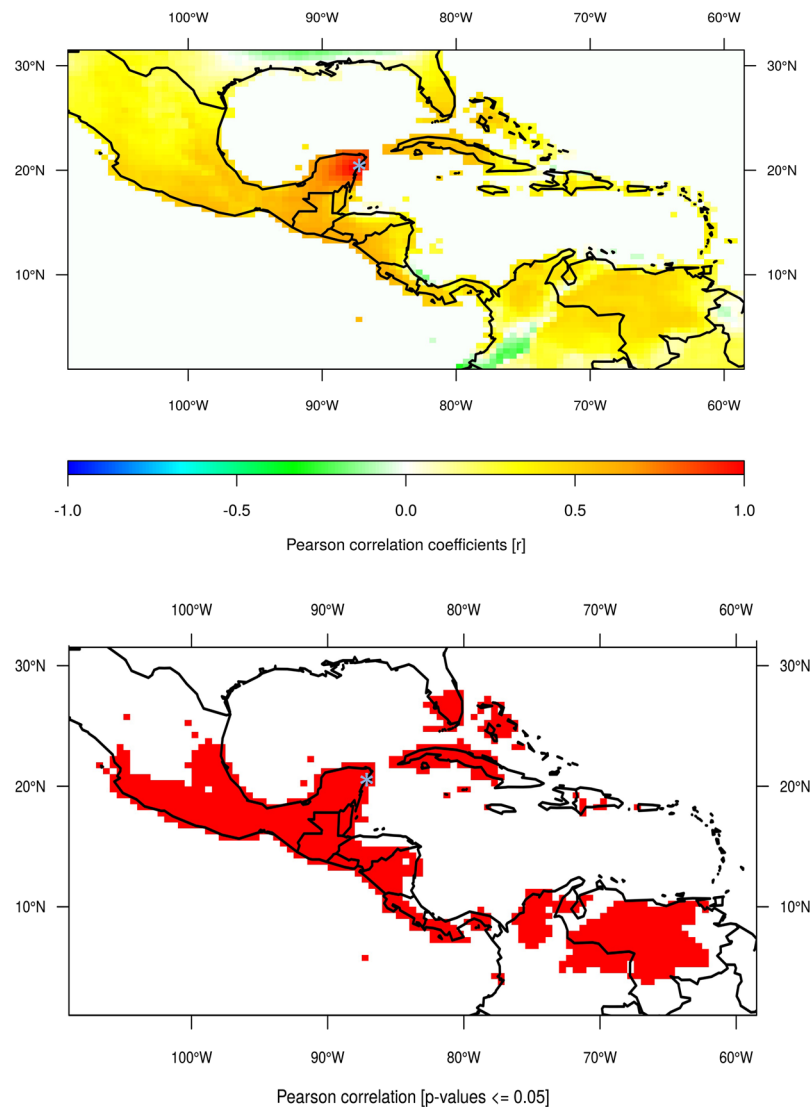


**Figure 1.** Spatio-temporal correlation analysis of precipitation (monthly values from 01/1901 to 12/2013 and with a spatial coverage of  $0.5^\circ$  latitude by  $0.5^\circ$  longitude) at the location ( $20^\circ 15'N$ ,  $87^\circ 45'W$ ) (close to Playa del Carmen, Yucatan, Mexico). Location of Rio Secreto indicated with light blue asterisk. The precipitation data set comes from the GPCC Global Precipitation Climatology Centre and is available from <https://www.esrl.noaa.gov/psd/data/gridded/data.gpcc.html>. The map was created using the R software<sup>72</sup>.

Itzamna precipitation record variability on multidecadal time scales, 32–64 years, may reflect a potential connection with the dominant pattern of North Atlantic sea surface temperature (SST) associated with the Atlantic Multidecadal Oscillation (AMO)<sup>33–35</sup>. Instrumental, paleoclimate and modeling data support a link between AMO and hydroclimate variability over large parts of the North Atlantic<sup>35, 36</sup>, African Sahel<sup>37, 38</sup>, western Europe<sup>36, 39, 40</sup>, northeastern Brazil<sup>37</sup>, Cuba<sup>41</sup> and North America<sup>42, 43</sup>. Particularly for the Gulf of Mexico and Caribbean regions, model simulations and analyses of instrumental data suggest a positive correlation between precipitation and the phases of AMO<sup>36, 44</sup>. Large-scale hydrological responses to AMO have been associated with variations in the SST gradient between the north and south Atlantic<sup>40, 45</sup>, shifts in the mean Intertropical convergence zone (ITCZ)<sup>36</sup> and changes in Atlantic tropical cyclogenesis<sup>36, 46</sup>.

Higher frequency variability at an ~8 year period in the Itzamna precipitation record may reflect El Niño–Southern Oscillation (ENSO) modulation of Caribbean hydroclimate (Fig. 2A). Studies with models and historical records suggest that Caribbean precipitation regimes are modulated by ENSO<sup>47–49</sup> and there is evidence that this modulation could be via the influence of ENSO on tropical Atlantic cyclogenesis<sup>23, 50</sup>. Atlantic hurricanes are suppressed when El Niño conditions in the Pacific induce upper altitude increased wind shear in the Atlantic, thus reducing rainfall fluxes over the YP by tropical cyclones<sup>51, 52</sup>.

Interannual and multidecadal variability (~8–128 year periods) is also suggested by four other stalagmite  $\delta^{18}O$  records spanning the Late Holocene from the YP<sup>23, 53</sup>, Belize<sup>50, 54</sup> and Cuba<sup>41</sup> and by last glacial lacustrine paleoenvironmental records from Lake Petén Itzá<sup>6, 55, 56</sup>. Observed and inferred hydrological change in the Caribbean and

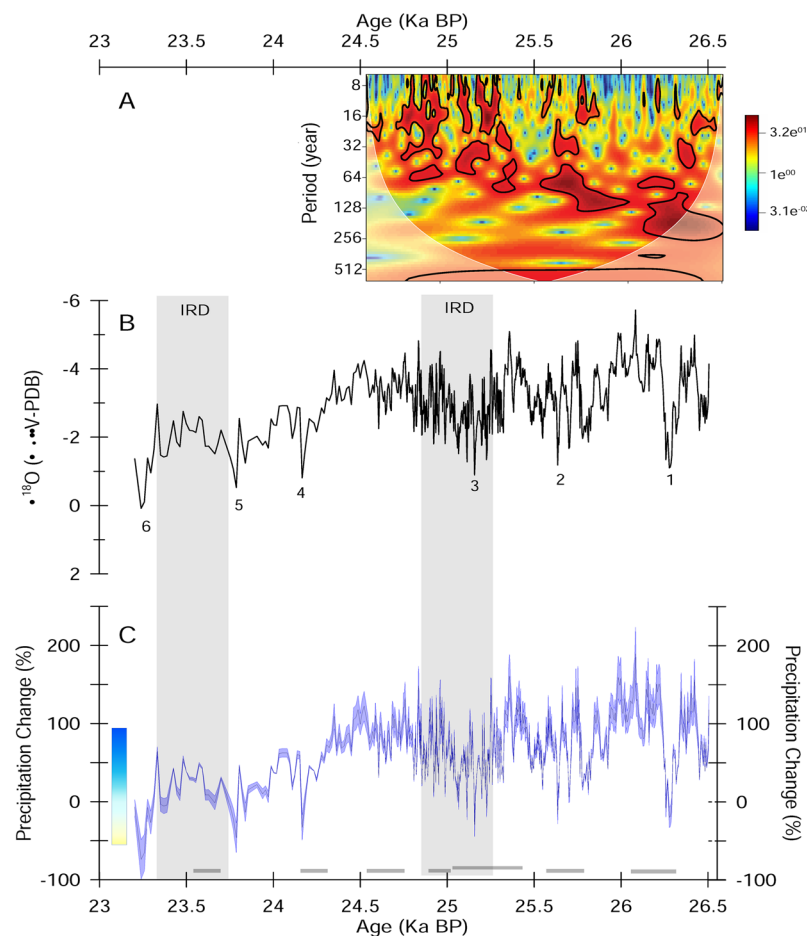


**Figure 2.** Itzamna  $\delta^{18}\text{O}$  (panel B) and  $\delta^{18}\text{O}$ -derived precipitation (panel C) records spanning the time interval between 26.4 and 23.2 ka BP from Rio Secreto, Playa del Carmen, Mexico. Precipitation percent change estimates are relative to the mean annual precipitation amount in Playa del Carmen today of 1465 mm (panel B). These records have a resolution during the time interval between 26.5 and 24.6 ka BP of  $3.4 \pm 1.3$  years (1 SD) and between 24.6 and 23.2 ka BP of  $16 \pm 6.7$  years (1 SD). Precipitation change estimates (blue shading) reflect reference values of calcite precipitated under isotopic equilibrium conditions with last glacial dripwater temperature ( $18\text{--}20^\circ\text{C}$ ) and an amount effect ( $\delta P/\Delta P$ ) ranging from  $-0.0168\%$  per mm to  $-0.0106\%$  per mm, corresponding to the 80% confidence interval of the amount effect slope based on instrumental data (see Methods section for more details). Average precipitation change is indicated by the blue line within blue shading. Reference equilibrium values were calculated using the paleotemperature equation by ref. 32. The potential bias in our precipitation estimates due to shifts in annual precipitation amount seasonality is  $\pm 8\%$  in the range of 55 to 70% summer contribution to annual precipitation (see Methods section). Vertical box on the left of panel B; indicates precipitation variability observed today in the northeast of the YP (mean = 1390 mm per year; range 670 mm to 2664 mm per year), based on the longest continuous instrumental record of precipitation available for this region (i.e. Kantunilkil Station)<sup>21</sup>. The record covers Stadial 2 and Heinrich event 2 (H2). Vertical grey bars reflect the two peak IRD depositional phases associated with H2, centered at  $25 \pm 0.2$  ka BP and  $23.5 \pm 0.2$  ka BP<sup>13</sup>. The six significant positive  $\delta^{18}\text{O}$  shifts discussed in the manuscript are indicated with numbers. Top image (panel A), represents a wavelet spectral power analysis of the Itzamna  $\delta^{18}\text{O}$  record. The area outside the white lines indicates the cone of influence where the edge effects of the wavelet transform and uncertainties become important and the black contours reflect statistically significant power spectra (CI = 95%). Wavelet spectral power is based on methods by refs 73, 74, as implemented in the R package “biwavelet”<sup>72</sup>.

Gulf of Mexico regions during the Holocene and last glacial intervals indicate that Atlantic low latitude regions respond to internal modes of climate variability on interannual (i.e. ENSO) and multidecadal time scales (i.e. AMO) regardless of the global climate state (i.e. interglacial versus glacial conditions).

As previously described, the Itzamna precipitation record suggests a significant long-term drying trend that began approximately 24.5 ka BP, following estimated precipitation mean maximum levels of  $+150\%$  and humid conditions in Central America<sup>6,55</sup>. This drying trend ended about 23.2 ky ago when mean precipitation declined by about 50% (based on the average of the three most recent data points) and the stalagmite Itzamna became ‘dormant’ for 20 thousand years. This declining precipitation trend coincides with a reduction in Itzamna

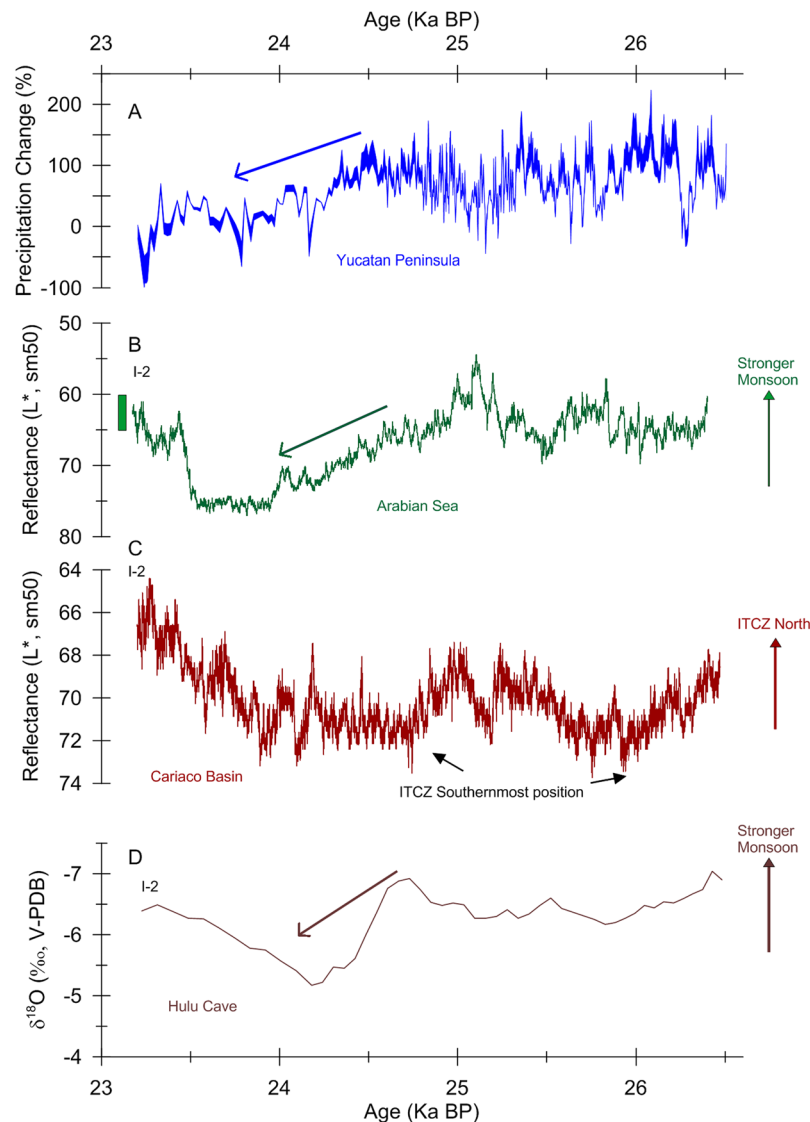


**Figure 3.** (A) Itzamna stalagmite precipitation record (this study), (B) northeastern Arabian sea sediment reflectance  $L^*$  record<sup>8</sup> and (C) Cariaco Basin, northern Venezuela, sediment reflectance  $L^*$  record<sup>8</sup>. Arrows illustrate weakening of YP precipitation and Indian monsoon. Green vertical bar in panel B represents the Arabian Sea sediment reflectance range reflecting Holocene values. This range illustrates that the intensity of the Indian Monsoon was not significantly different in the early stages of S2 than during the Holocene. For reference, Cariaco Basin sediment  $L^*$  reflectance values associated with previous stadial episodes (e.g. stadials 3–18) were lower than the lowest S2 values, thus suggesting that the Atlantic ITCZ was not particularly displaced south during S2 relative to a typical stadial. Differences in the timing of interstadial 2 among these records reflect chronological uncertainties >200 years<sup>4,8</sup>.

speleothem growth thus reinforcing the isotopic evidence for precipitation declines (Fig. S3). A long-term shift from high to low precipitation regimes at ~24.5 ka BP is also suggested by other northern and, interestingly, southern hemisphere climate records. In the northern hemisphere, this climate transition occurs at ~24.6 ka BP in the speleothem monsoon  $\delta^{18}\text{O}$  record from Hulu Cave in Eastern China (32°30'N, 119°10'E)<sup>4</sup> and at ~24.7 ka BP in an ocean sediment total reflectance  $L^*$  record from the northeastern Arabian Sea (23°07.34'N, 66°29.84'E)<sup>8</sup> (Fig. 3). In the southern hemisphere, a similar climate transition occurs at ~24.4 ka BP in a speleothem  $\delta^{18}\text{O}$  record from Pacupahuain Cave in the central Peruvian Andes (11.24°S, 75.82°W)<sup>7</sup> and at ~24.8 ka BP in a speleothem  $\delta^{18}\text{O}$  record from Paraiso Cave in the Amazon basin (4°4'S, 55°27'W)<sup>15</sup> (Fig. 4). The Cariaco Basin sediment total reflectance record (10°40.69'N, 64°58.29'W)<sup>8</sup>, interpreted to reflect the mean position of the ITCZ, also shows a transition from low to high reflectance values at the time (Fig. 3). Together, these observations would suggest that the coeval change in the Cariaco Basin sediment reflectance record probably reflects a decrease in the intensity of tropical convective activity and not a significant shift in the ITCZ position as would be observed over stadial-to-interstadial transitions (Figs 3 and 4). We want to point out that the observation of synchronous and in-phase precipitation reduction in the American tropics during stadial 2 does not contradict evidence for

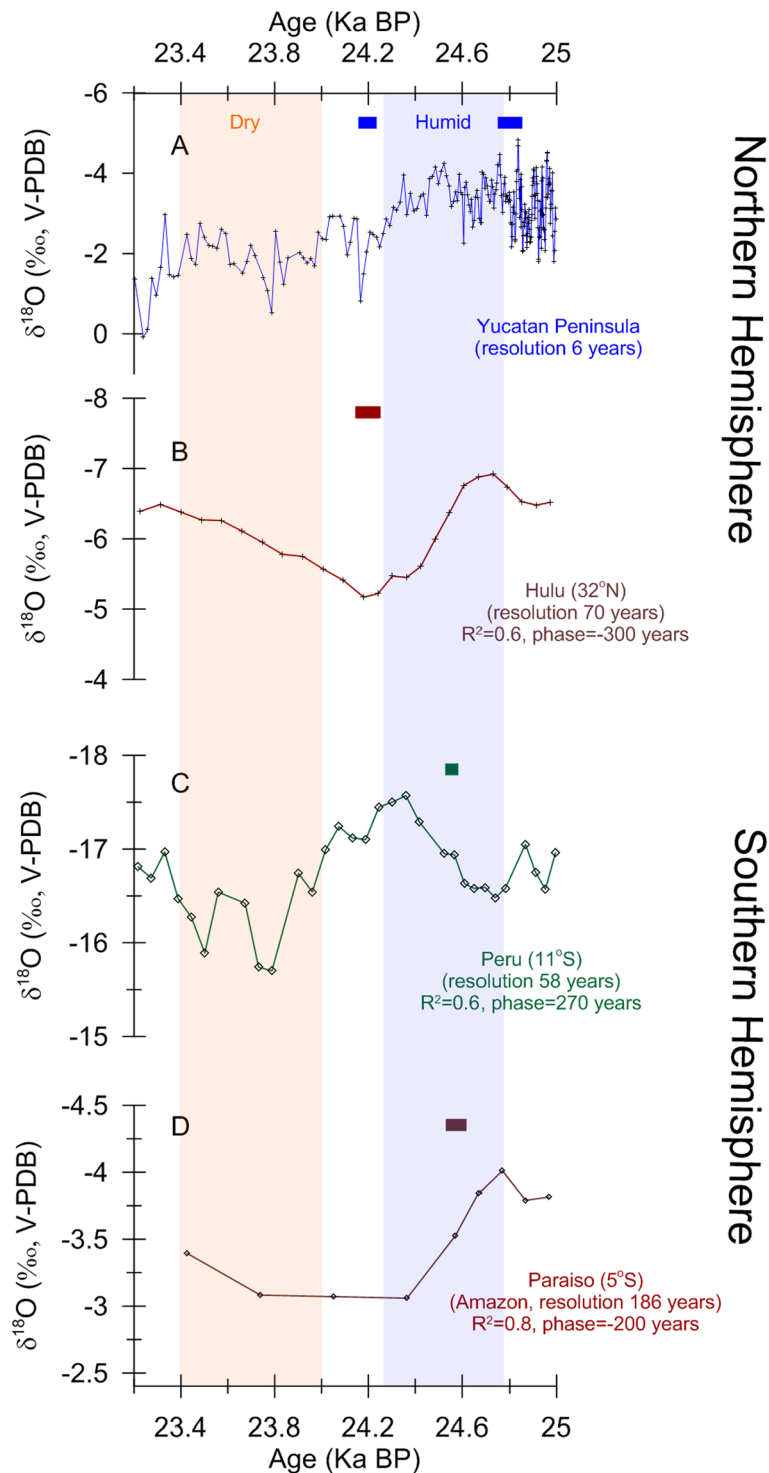


**Figure 4.** Blow up comparing speleothem  $\delta^{18}\text{O}$  records from the northern and the southern Hemispheres between 25 and 23.2 ka BP. Speleothem  $\delta^{18}\text{O}$  record from the Yucatan Peninsula (20°N) (A), Hulu, China (32°N)<sup>4</sup> (B), Perú (11°S)<sup>7</sup> (C), and Paraíso, Amazon Basin (5°S)<sup>15</sup> (D). The time resolution of these records is shown. Cross-correlation coefficient ( $r^2$ ) and phase relationship between the YP speleothem  $\delta^{18}\text{O}$  record and the other speleothem  $\delta^{18}\text{O}$  records are shown. Negative/positive phase values represent that the YP  $\delta^{18}\text{O}$  record lags/leads the other speleothem  $\delta^{18}\text{O}$  records, respectively. These records are in phase within their combined age uncertainties. Small color box above each record shows the U-Th age and its uncertainty (2 Sigma) available for each record within this time interval (Itzamna =  $\pm 73$  years; Hulu =  $\pm 100$  years; Perú =  $\pm 50$  years; Paraíso =  $\pm 84$  years). Vertical color bars illustrate the transition from humid to drier conditions as suggested by these speleothem  $\delta^{18}\text{O}$  records reflecting precipitation amount.

an anti-phase precipitation relationship on stadial-interstadial time scales, which is supported by a number of studies<sup>7,8,14,15</sup>. The Itzamna record spans stadial 2 and thus we cannot infer precipitation conditions during the following or preceding interstadial time intervals and detect the anti-phase relationship during full D-O events that is revealed by tropical paleoclimate records.

The hydrological response across the American tropics occurs during the onset and duration of H2. Magnetic susceptibility and mineralogical records from the high-resolution (20 cm/1000 year) Iberian Margin Core SU8118, one of the best-dated sediment records of H2, suggest two IRD depositional phases centered at  $23.5 \pm 0.2$  ka BP and  $25 \pm 2$  ka BP<sup>13</sup>, in agreement with other assessments of H2 based on sediment cores from the North Atlantic<sup>12</sup> (Fig. 2). These depositional phases occurred in association with cooling and advection of low-salinity arctic water masses in the subtropical Atlantic, as suggested by alkenone records from core SU8118<sup>13</sup>.

Progressive precipitation decline in the YP (this study), Central America<sup>6,55</sup>, India and South East Asia, coeval with precipitation reduction in Perú<sup>7</sup> and the Amazon Basin<sup>15</sup>, associated with H2, are consistent with model results of AMOC slowdown. Particularly, hosing experiments based on atmosphere–ocean general circulation models suggest that freshening of the North Atlantic and the ensuing AMOC slowdown and atmospheric cooling would cause significant precipitation reduction in the American tropics, including the Caribbean and Amazon basin<sup>16,17</sup>. Notably, the magnitude of precipitation decline during the most intense rainfall reduction events suggested by the Itzamna record of  $\sim 50\%$  is consistent with model results of peak precipitation reduction in the Caribbean region associated with AMOC slowdown<sup>16</sup>.

We suggest that extreme drought conditions in the YP after  $\sim 24.5$  ka BP was an inevitable pattern that followed high regional precipitation in the Caribbean and warm ocean anomalies in the North Atlantic, the latter possibly related to a positive AMO phase. North Atlantic warming and freshening combined would trigger massive iceberg discharges into the North Atlantic (i.e. H2) and the resulting meridional propagation of cooling via advection and air–sea interactions<sup>19</sup> would then cause a reduction in low latitude rainfall<sup>16</sup>. The North Atlantic low latitude precipitation reduction by the end of S2 was intense enough to have likely played a counteracting role to AMOC slowdown. North Atlantic high salinity induced by intense low latitude precipitation deficits, as the Itzamna precipitation record suggests, would propagate to the high latitudes, increase upper ocean convection, and help resume AMOC, as proposed by previous studies<sup>57–59</sup>. A recent study that investigates the northward flow of warm water through the Florida Strait, from benthic foraminiferal  $\delta^{18}\text{O}$  records from sediment cores, does not find evidence of significant shifts in the Atlantic overturning circulation during H2<sup>60</sup>. The implication of these findings by ref. 60 is that precipitation reductions in the YP and presumably in the northern Caribbean region resulting from the meridional propagation of cooling during H2 may have helped counteract AMOC slowdown during this time.

The Arabian Sea and Cariaco Basin sediment reflectance values during S2 are the lowest of all stadial events, thus suggesting to be the wettest of all stadial events, and comparable to values observed during interstadials 9, 18 and 20 within these records. These observations suggest that the ITCZ was not particularly displaced south during S2. The evidence presented thus far implies that cooling associated with Heinrich events can significantly impact tropical and subtropical hydroclimate during stadials without involving a shift in the mean position of the ITCZ. In the specific case of S2, Atlantic cooling could have induced lower precipitation across the tropical Americas by decreasing the atmosphere's moisture holding capacity and, by decreasing the intensity of tropical convection<sup>16</sup>. Tropical Atlantic cyclogenesis was also likely reduced during the last glacial and particularly during cool stadial episodes, when tropical convection and SSTs in the main developmental region were reduced<sup>61</sup>. Precipitation reductions in the Caribbean region during S2 could have thus been amplified by a lower potential of tropical cyclones to transfer moisture to higher latitudes<sup>46,62</sup>.

This work provides new high-resolution stalagmite  $\delta^{18}\text{O}$  and  $\delta^{18}\text{O}$ -derived precipitation records that help characterize the magnitude and frequency of Caribbean hydroclimate variability on interannual and multidecadal time scales during a stadial event. Our study offers new evidence that precipitation across the American tropics declined progressively in close association with the onset and duration of Heinrich event 2. The geographical pattern and magnitude of tropical hydrological change during stadial 2 suggested by paleoclimate records, furthermore, are consistent with model results of AMOC slowdown. We propose that increased salinity in the Caribbean region driven by a precipitation deficit resulting from North Atlantic cooling associated with H2 played a crucial role in helping counteract AMOC slowdown. In light of the evidence provided, we suggest that tropical hydroclimate does not only respond to but also influences AMOC circulation during glacial intervals, in agreement with previous studies<sup>57–59</sup>.

Lastly, we suggest that the Itzamna stalagmite precipitation estimates be considered as preliminary and not as an end result. We anticipate that modeling studies will help expand our understanding of the amount effect and the isotopic composition of precipitation during the last glacial and thus help test our precipitation inferences. The long-term monitoring of precipitation we are conducting will reveal the robustness of the link between tropical precipitation amount and precipitation  $\delta^{18}\text{O}$  on interannual time scales revealed by models<sup>22</sup>, while helping us understand the factors that control this relationship and those that may disrupt it, such as tropical cyclones<sup>63</sup>. Speleothems from tropical regions may represent our best chance to reconstruct low latitude precipitation variability and its sensitivity to shifts in climate boundary conditions (e.g. greenhouse gases) and processes internal to the climate system (e.g. AMOC).

## Methods

**U-Th dating.** Calcite powders weighing from 0.1 to 0.15 g were used for U-Th chemistry<sup>24</sup>. Uranium and thorium isotopic measurements were conducted on a multi-collector inductively coupled plasma mass spectrometer (MC-ICP-MS), Thermo Fisher Neptune, at the High-Precision Mass Spectrometry and Environment Change Laboratory (HISPEC), Department of Geosciences, National Taiwan University<sup>26</sup>. A triple-spike,  $^{229}\text{Th}$ – $^{233}\text{U}$ – $^{236}\text{U}$ , isotope dilution method was employed to correct for mass bias and determine all uranium and thorium isotopic

and concentration values in an off-line data reduction process developed by ref. 64. All errors of isotopic data and dates given (Table S1) are two standard deviations (Supplementary materials Fig. S7). We developed the chronology of this section based 2000 Montecarlo simulations using the COPRA software<sup>27</sup> (Table S2).

Calcite  $\delta^{18}\text{O}$  analyses were performed at the University of Massachusetts using an on-line carbonate preparation system linked to a Finnigan Delta Plus XL isotope ratio mass spectrometer. Reproducibility of the standard materials is better than  $\pm 0.1\text{‰}$ . Values are reported relative to the V-PDB standard.

**Cave Monitoring.** We monitored relative humidity daily in two sectors of Río Secreto including at the stalagmite Itzamna collection site during two full years, from June 2014 to June 2016 ( $n = 5000$  measurements using HOBO instruments). Relative humidity of 100% was recorded throughout this time. The cave floor is currently below the water table and thus provides a constant moisture source that is particularly retained in cave chambers. We recognize that these conditions were likely different during the last glacial when sea level and thus the water table in the cave were much lower than today. Cave relative humidity during the last glacial may have remained, however, close to 100% because of lower evaporation resulting from global cooling. In addition, we have monitored caves with no standing water inside in the northwest most arid region of the YP<sup>53</sup> and found relative humidity at or near saturation levels. We monitored cave temperature inside the chamber of Itzamna, known as Laberinto del Fauno, for 1.5 years from June 2015 to October 2016 ( $n > 1787$  measurements using HOBO instruments). Measured cave air temperature inside this chamber was  $23 \pm 1^\circ\text{C}$  thus reflecting  $3^\circ\text{C}$  colder mean temperature than the annual mean air temperature in Playa del Carmen of  $26^\circ\text{C}$ <sup>21</sup>. In June 2014 we initiated a weekly collection of drip waters from different stalactites in various chambers within the cave system. Results from 163 dripwater measurements taken between the year 2014 and 2016 indicate an average drip water  $\delta^{18}\text{O}$  composition of  $-3.7 \pm 1.0\text{‰}$  in Laberinto del Fauno. The observed drip  $\delta^{18}\text{O}$  variability was in tune with the seasonal cycle of precipitation consistent with a relatively short mixing time of drips<sup>23</sup>. The mean drip water  $\delta^{18}\text{O}$  value ( $-3.7 \pm 1.0\text{‰}$ ) is very similar to the annual amount weighted  $\delta^{18}\text{O}$  value ( $-4\text{‰}$ ) of rainfall in Playa del Carmen during this interval of time ( $n = 13$  months). Modern dripwater temperature in this chamber is  $23^\circ\text{C}$ , based on 1.2 years of weekly measurements of two drips ( $n = 62$  weeks). These observations suggest that it is unlikely for evaporation to significantly influence dripwater geochemistry at these sites. Measured Laberinto del Fauno dripwater and groundwater temperatures are similar to the cave air temperature ( $23 \pm 1^\circ\text{C}$ ). Similar cave air, dripwater and groundwater temperatures that are  $3^\circ\text{C}$  colder than the mean annual surface air temperature suggests that dripwater temperature reflects cave air temperature and this in turn groundwater temperature because groundwater is present year round in the Río Secreto cave system.

**Amount effect.** Instrumental records of precipitation amount and rainfall  $\delta^{18}\text{O}$ , and modeling studies, indicate that there is an amount effect on seasonal and interannual time scales in the Yucatan Peninsula<sup>22, 23</sup>. We have previously characterized the seasonal amount effect between precipitation amount ( $P$ ) and precipitation  $\delta^{18}\text{O}$  ( $dP$ ) by monitoring rainfall amount and rainfall  $\delta^{18}\text{O}$  in the city of Cancún in the year 2012 and in Río Secreto in 2014<sup>23</sup>. The amount effect on seasonal time scales in the YP is represented by the slope  $dP/\Delta P = -0.0137 \pm 0.0031\text{‰/mm}$  (80% confidence interval, CI,  $r = 0.87$ ). The amount effect is statistically similar (80% CI) to that recorded in Veracruz, México ( $-0.0125\text{‰ per mm}$ ), in San Salvador, El Salvador ( $-0.0124\text{‰ per mm}$ )<sup>23, 65</sup>, Havana, Cuba ( $-0.0147\text{‰ per mm}$ ) and Tuscaloosa, Alabama ( $-0.0132\text{‰ per mm}$ ) (GNIP, IAEA). We currently have no means to assess the value of the amount effect in the YP during the last glacial time interval. The similar amount effect slope found in the northern Caribbean and Gulf of Mexico regions suggest that this parameter is relatively stable across different climate regimes. In order to include a measure of uncertainty regarding the amount effect, this study uses the full confidence interval of the amount effect slope measured in the northeast of the YP to calculate precipitation changes. The slope range (i.e.  $-0.0168$  and  $-0.0106\text{‰ per mm}$ ) well exceeds values observed in northern Caribbean and Gulf of Mexico locations today.

**Expected equilibrium stalagmite  $\delta^{18}\text{O}$  values.** Oxygen isotope data from Río Secreto indicate that dripwater  $\delta^{18}\text{O}$  composition closely reflects the annual amount-weighted  $\delta^{18}\text{O}$  composition of rainfall<sup>23</sup>. Applying the equation by Tremaine *et al.*<sup>32</sup>, we calculate the expected stalagmite  $\delta^{18}\text{O}$  composition precipitated under oxygen isotopic equilibrium conditions with cave dripwater annual temperature ( $23^\circ\text{C}$ ), by using the local amount effect relationship characterized instrumentally ( $Y = -0.0137x - 0.9525$ ), and 5-year monthly averages of precipitation amount (1998–2003,  $1465 \pm 280$  mm/yr). The equilibrium calculations yield a stalagmite  $\delta^{18}\text{O}$  composition of  $-4.1\text{‰}$ , which is within the variability range of the most recent section of Itzamna ( $-4.8 \pm 1.3\text{‰}$ , 2 SD) spanning the Preclassic Period of Maya history (BCE 1037 to CE 397)<sup>23</sup>. The Itzamna record we present in this study has a mean  $\delta^{18}\text{O}$  composition of  $-3.1\text{‰} \pm 1.8\text{‰}$  (2 SD), that is,  $1.7\text{‰}$  more positive than the mean  $\delta^{18}\text{O}$  composition of the younger section (Fig. S8). Comparisons of Holocene and Last glacial speleothem  $\delta^{18}\text{O}$  records would suggest that the YP was drier during the last glacial relative to the Holocene, even when considering a last glacial positive shift in ocean  $\delta^{18}\text{O}$  of  $1\text{‰}$  due to the expansion of high latitude ice sheets<sup>66</sup>. Glacial temperature and rainfall  $\delta^{18}\text{O}$ , however, also need to be taken into account when comparing Holocene and glacial stalagmite  $\delta^{18}\text{O}$  values.

**Principle for quantitative precipitation estimates.** Precipitation  $\delta^{18}\text{O}$  is controlled by precipitation amount on seasonal and interannual time scales in the YP, therefore, if it rains the same amount in five consecutive years, the precipitation  $\delta^{18}\text{O}$  composition (amount weighted) is expected to remain unchanged. If precipitation amount changes on one given year, then precipitation  $\delta^{18}\text{O}$  would change according to the amount effect relationship. Precipitation estimates from stalagmite  $\delta^{18}\text{O}$  represent the average precipitation amount of one, two or the number of years our sample integrates. Depending on the site, seasonal dripwater  $\delta^{18}\text{O}$  could conceivably integrate the annual precipitation isotopic signal, as we observe in some drips from Río Secreto, in which case, stalagmite  $\delta^{18}\text{O}$  would closely represent an annual precipitation  $\delta^{18}\text{O}$  signal integration (albeit with some delay),

even when it is sampled on seasonal resolution. Because stalagmite  $\delta^{18}\text{O}$  per mil shifts are assumed to reflect similar shifts in precipitation  $\delta^{18}\text{O}$ , interannually, we can then estimate precipitation amount shifts from stalagmite  $\delta^{18}\text{O}$  anomalies calculated relative to a reference point. We maintain the local modern annual precipitation cycle but shift annual precipitation amount and therefore precipitation  $\delta^{18}\text{O}$  so that annual mean precipitation  $\delta^{18}\text{O}$  changes in accordance to the interannual  $\delta^{18}\text{O}$  precipitation anomalies reflected by the stalagmite<sup>30</sup>. Seasonality may produce precipitation amount biases on both directions, positive and negative, using this method. Summer precipitation to total annual precipitation on typical years today in the northeast YP range from a minimum of 60% to a maximum of 70% summer precipitation (Fig. S2). We estimated how much these shifts in seasonality associated with the same amount of annual precipitation would affect our precipitation inferences. The potential seasonal precipitation bias in our estimates is  $\pm 8\%$ , within the range of 55 to 70% summer contribution to annual precipitation; a 5% larger seasonality than observed today.

**Quantification of precipitation amount from Itzamna during the last glacial.** We use the 5-year annual mean of precipitation (1998–2003) in Playa del Carmen of 1465 mm as the reference precipitation value for our estimates of precipitation change<sup>23</sup>. The last glacial equilibrium  $\delta^{18}\text{O}$  composition of Itzamna ( $\delta^{18}\text{O}_{\text{c-PDB}}$ ) for this reference value is calculated with the paleotemperature equation by ref. 32:

$$t(^{\circ}\text{C}) = 1000 / (((1000 * \ln \alpha) + 24.6) / 16.1)$$

where  $\alpha = (1000 + \delta^{18}\text{O}_{\text{c-VSMOW}}) / (1000 + \delta^{18}\text{O}_{\text{w-VSMOW}})$  and  $\delta^{18}\text{O}_{\text{c-VSMOW}} = 30.92 + 1.03092 * (\delta^{18}\text{O}_{\text{c-PDB}})$ .

Here the last glacial cave dripwater  $\delta^{18}\text{O}$  composition ( $\delta^{18}\text{O}_{\text{w-VSMOW}}$ ) in Río Secreto is determined from assuming the annual  $\delta^{18}\text{O}$  composition of precipitation (amount-weighted) associated with 1465 mm/yr (reference value). This assumption is supported by instrumental monitoring data as detailed above<sup>23</sup>. The last glacial annual  $\delta^{18}\text{O}$  composition of precipitation (amount-weighted) was determined from adjusting a 1.6‰ higher last glacial annual precipitation  $\delta^{18}\text{O}$  value relative to today, as suggested by global circulation models GCMs<sup>67, 68</sup>. We want to point out that because few studies exist that investigate shifts in precipitation  $\delta^{18}\text{O}$  during glacial intervals, it is difficult to assess how certain/uncertain this adjustment of precipitation  $\delta^{18}\text{O}$  may be, although a minimum of  $\sim 1.2\%$  positive shift in precipitation is expected as a result of the last glacial shift in ocean  $\delta^{18}\text{O}$  due to expansion of the continental ice sheets<sup>66</sup>. Evidently, interpretations of speleothem  $\delta^{18}\text{O}$  records from tropical regions would greatly benefit from increasing development of studies focused on isotope-enabled GCMs that target glacial conditions.

The S2 temperature of dripwaters ( $t$ ) was calculated by subtracting a tropical glacial cooling of 3–5 °C that is suggested by seven Atlantic tropical SST records<sup>31</sup> from the modern mean annual dripwater temperature of 23 °C. We note that, this Holocene-to-last glacial SST range also applies to the Arabian Sea, Indian Ocean and tropical Pacific<sup>31</sup>. We consider this 2 °C temperature range as uncertainty associated with our estimates of last glacial cave temperature. This yields a final dripwater temperature estimate ranging from 18 °C to 20 °C. The resulting equilibrium  $\delta^{18}\text{O}$  composition of calcite associated with last glacial conditions and 1465 mm/year ranged from  $-1.4\%$  at 18 °C to  $-1.7\%$  at 20 °C.

Stalagmite  $\delta^{18}\text{O}$  anomalies were then calculated in reference to these two isotopic equilibrium values. Positive and negative  $\delta^{18}\text{O}$  anomalies would therefore indicate lower and higher precipitation relative to 1465 mm, respectively. Precipitation percent changes were then calculated based on the full confidence interval of the slope of the relationship between the amount of precipitation and precipitation  $\delta^{18}\text{O}$  ( $\delta P / \Delta P = -0.0137 \pm 0.0031\%$  per mm), equivalent to the slopes  $-0.0106\%$ /mm and  $-0.0168\%$ /mm. As expected, the steepest slope will yield the lowest precipitation change associated to a given  $\delta^{18}\text{O}$  anomaly. As an example, a positive stalagmite anomaly of +1‰ would be explained by shifting precipitation amount and therefore the annual cycle of precipitation  $\delta^{18}\text{O}$  (last glacial adjusted) by  $-55\%$  and  $-35\%$ , using the slopes  $-0.0106\%$ /mm and  $-0.0168\%$ /mm, respectively. We note that the precipitation estimates associated with a stalagmite  $\delta^{18}\text{O}$  anomaly, for instance of +1‰, depend on the reference value. If we increased 50% the reference value 1465 mm to 2194.5 mm, then a +1‰ anomaly would be explained by annual precipitation amount reductions of  $-38\%$  and  $-24\%$  using the slopes  $-0.0106\%$  per mm and  $-0.0168\%$  per mm, respectively.

We used the paleotemperature equation by Tremaine *et al.*<sup>32</sup> because this equation applies to a broad range of temperature and cave environments. We explored the alternative paleotemperature equation by Kim and O'Neil<sup>69</sup> and found that precipitation estimates not based on the steepest slope ( $-0.0168\%$ /mm) yielded precipitation declines in excess of 100%. Precipitation declines  $> 100\%$  would not support this equation, or suggest that the amount effect was similar or higher than  $-0.0168\%$  per mm during S2. Alternatively, excess precipitation declines could indicate underestimation of the last glacial precipitation  $\delta^{18}\text{O}$  shift, underestimation of the magnitude of cooling, and/or calcite disequilibrium precipitation during peak drought. The last glacial precipitation  $\delta^{18}\text{O}$  shift that would explain the most positive stalagmite  $\delta^{18}\text{O}$  value (0.1‰) without resulting in precipitation declines in excess of 100% over the temperature and amount effect conditions applied is 2.4‰, which is 0.8‰ more positive than the value suggested by climate model results (1.6‰)<sup>67, 68</sup> and  $\sim 1.2\%$  more positive than explained by a shift in ocean  $\delta^{18}\text{O}$  associated with the expansion of the continental ice sheets<sup>66</sup>. A larger precipitation  $\delta^{18}\text{O}$  adjustment is therefore unsupported by available model results and paleoclimate proxy records. Examination of available last glacial subtropical and tropical Atlantic sea surface temperature records<sup>70, 71</sup>, on the other hand, does not suggest Caribbean sea glacial cooling larger than 5 °C. Lastly, we cannot discard disequilibrium isotopic conditions during peak drought events induced by decreasing cave relative humidity. The atmospheric demand of moisture and thus evaporation, however, were lower during the last glacial due to regional cooling<sup>61</sup>, which would have helped maintain water vapor saturation conditions inside the cave.

Based on the available evidence, we find stronger support for applying the paleotemperature equation by Tremaine *et al.*<sup>32</sup>, which applies to a broad range of cave temperatures and environments similar to Río Secreto,

and does not produce precipitation declines in excess of 100% across the range of temperatures and amount effect slopes applied in this study. Additional precipitation records and the long-term monitoring we are currently conducting in Rio Secreto, involving farmed calcite, will provide more definite support for our chosen paleotemperature equation.

**Assessment of influence of chronological uncertainty on spectral analysis.** In order to assess chronological uncertainty effects on our spectral results, we expand and contract the time scale over periods of interest and determine how this affects the duration of the dominant periods suggested by the spectral analysis (Fig. 2A). Specifically, the period of variability that may reflect ENSO variability, centered at ~8 years, is particularly strong over a 700-year time interval between 24.7–25.4 kyr BP. We thus expand and contract the time scale over this time interval by applying the average radiometric age uncertainty ( $\pm 132$  years) and then determine how the dominant period of variability of 8 years would be affected. This analysis yields a dominant period of 9.5 and 6.5 years on the expanded and contracted time scales, respectively. Chronological uncertainties, therefore, translate into a dominant period of variability of  $8 \pm 1.5$  years. Regarding multidecadal time scales and the periods of variability centered at 32 and 64 years, we use the entire interval of 1542 years represented by the spectral analysis plot and expand and contract this time scale by the maximum age uncertainty of  $\pm 202$  years. This assessment yields periods of variability of  $32 \pm 4$  years and  $64 \pm 8$  years, thus suggesting that chronological uncertainties have little influence on the duration of the dominant periods of variability suggested by our spectral analysis.

## References

- Dansgaard, W. *et al.* North Atlantic climatic oscillations revealed by deep Greenland ice cores. Vol. 29, 3–8 (American Geophysical Union, 1984).
- Oeschger, H. *et al.* Late glacial climate history from ice cores. Vol. 29 299–306 (American Geophysical Union, 1984).
- Hendy, I. L. & Kennett, J. P. Dansgaard-Oeschger cycles and the California Current System: Planktonic foraminiferal response to rapid climate change in Santa Barbara Basin. *Paleoceanography* **15**, 30–42 (2000).
- Wang, Y. J. *et al.* A high-resolution absolute-dated Late Pleistocene monsoon record from Hulu Cave, China. *Science* **294**, 2345–2348, doi:<https://doi.org/10.1126/Science.1064618> (2001).
- Peterson, L. C., Haug, G. H., Hughen, K. A. & Röhl, U. Rapid Changes in the Hydrologic Cycle of the Tropical Atlantic During the Last Glacial. *Science* **290**, 1947–1951 (2000).
- Hodell, D. A. *et al.* An 85-ka record of climate change in lowland Central America. *Quaternary Sci Rev* **27**, 1152–1165 (2008).
- Kanner, C. L., Burns, J. S., Cheng, H. & Edwards, R. L. High-Latitude Forcing of the South American Summer Monsoon During the Last Glacial. *Science* **335**, 570–573 (2012).
- Deplazes, G. *et al.* Links between tropical rainfall and North Atlantic climate during the last glacial period. *Nature Geoscience* **6**, 213–217 (2013).
- Broecker, W. S. & Denton, G. H. The role of ocean-atmosphere reorganizations in glacial cycles. *Geochim Cosmochim Acta*, 2465–2501 (1989).
- Clark, P. U. *et al.* Freshwater forcing of abrupt climate change during the last glaciation. *Science* **293**, 283–287 (2001).
- Heinrich, H. Origin and consequences of cyclic ice rafting in the northeast Atlantic Ocean during the past 130,000 years. *Quaternary Res* **29**, 142–152 (1988).
- Hemming, S. R. Heinrich events: massive late pleistocene detritus layers of the north Atlantic and their global climate imprint. *Reviews of Geophysics* **42** (2004).
- Bard, E., Rostek, F., Turon, J.-L. & Gendreau, S. Hydrological impact of Heinrich events in the subtropical northeast Atlantic. *Science* **289**, 1321–1324 (2000).
- Wang, X. *et al.* Millennial-scale precipitation changes in southern Brazil over the past 90,000 years. *Geophys. Res. Lett.* **34**, L23701 (2007).
- Wang, X. *et al.* Hydroclimate changes across the Amazon lowlands over the past 45,000 years. *Nature* **541**, 204–207 (2017).
- Otto-Bliesner, B. L. & Brady, E. C. The sensitivity of the climate response to the magnitude and location of freshwater forcing: last glacial maximum experiments. *Quaternary Sci Rev* **29**, 56–73 (2010).
- Lewis, S. C., LeGrande, A. N., Kelley, M. & Schmidt, G. A. Water vapour source impacts on oxygen isotope variability in tropical precipitation during Heinrich events. *Clim Past* **6**, 326–343 (2010).
- Stouffer, R. J. *et al.* Investigating the Causes of the Response of the Thermohaline Circulation to Past and Future Climate Changes. *Journal of Climate* **19**, 1365–1387 (2006).
- Chiang, J. C. H., Cheng, W. & Bitz, C. M. Fast teleconnections to the tropical Atlantic sector from Atlantic thermohaline adjustment. *Geophysical Research Letters* **35**, L07704 (2008).
- Andersen, K. K. *et al.* The Greenland Ice Core Chronology 2005, 15–42 ka. Part 1: constructing the time scale. *Quaternary Sci Rev* **25**, 3246–3257.
- CONAGUA. Servicio meteorológico nacional, México (available at: <http://smn.cna.gob.mx/>) (2012).
- Vuille, M. *et al.* Modeling delta O-18 in precipitation over the tropical Americas: 2. Simulation of the stable isotope signal in Andean ice cores. *J Geophys Res-Atmos* **108** (2003).
- Medina-Elizalde, M. *et al.* High-resolution speleothem record of precipitation from the Yucatan Peninsula spanning the Maya Preclassic Period. *Global Planet Change* **138**, 93–102 (2016).
- Shen, C.-C. *et al.* Measurement of attogram quantities of  $^{231}\text{Pa}$  in dissolved and particulate fractions of seawater by isotope dilution thermal ionization mass spectroscopy. *Analytical Chemistry* **75**, 1075–1079 (2003).
- Cheng, H. *et al.* Improvements in  $^{230}\text{Th}$  dating,  $^{230}\text{Th}$  and  $^{234}\text{U}$  half-life values, and U-Th isotopic measurements by multi-collector inductively coupled plasma mass spectrometry. *Earth Planet Sc Lett* **372**, 82–91 (2013).
- Shen, C.-C. *et al.* High-precision and high-resolution carbonate  $^{230}\text{Th}$  dating by MC-ICP-MS with SEM protocols. *Geochim Cosmochim Acta* **99**, 71–86 (2012).
- Breitenbach, S. F. M. *et al.* Constructing Proxy Records from Age models (COPRA). *Clim Past* **8**, 1765–1779 (2012).
- Sharp, Z. *Principles of Stable Isotope Geochemistry*. 344 (Pearson Prentice Hall, 2007).
- Rozanski, K., Araguás-Araguás, L. & Gonfiantini, R. In *Climate Change in Continental Isotopic Records*. (ed P. Swart, Lohmann, C., McKenzie, J. & Savin, S.) (Geophysical Monograph) (1993).
- Medina-Elizalde, M. & Rohling, E. J. Collapse of Classic Maya civilization related to modest reduction in precipitation. *Science* **335**, 956–959 (2012).
- Rohling, E. J., Medina-Elizalde, M., Shepherd, J. G., Siddall, M. & Stanford, J. D. Sea Surface and High-Latitude Temperature Sensitivity to Radiative Forcing of Climate over Several Glacial Cycles. *Journal of Climate* **25**, 1635–1656 (2012).
- Tremaine, D. M., Froelich, P. N. & Wang, Y. Speleothem calcite farmed *in situ*: Modern calibration of  $\delta^{18}\text{O}$  and  $\delta^{13}\text{C}$  paleoclimate proxies in a continuously-monitored natural cave system. *Geochim Cosmochim Acta* **75**, 4929–4950 (2011).

33. Bjerknes, J. Atlantic air–sea interaction. *Advances of Geophysics* **10**, 1–82 (1964).
34. Delworth, T. L. & Mann, M. E. Observed and simulated multidecadal variability in the Northern Hemisphere. *Climate Dynamics* **16**, 661–676 (2000).
35. Gray, S. T., Graumlich, L. J., Betancourt, J. L. & Pederson, G. T. A tree-ring based reconstruction of the Atlantic Multidecadal Oscillation since 1567 A.D. *Geophysical Research Letters* **31**, L12205 (2004).
36. Knight, J. R., Folland, C. K. & Scaife, A. A. Climate impacts of the Atlantic Multidecadal Oscillation. *Geophysical Research Letters* **33**, L17706 (2006).
37. Folland, C. K., Parker, D. E. & Palmer, T. N. Sahel rainfall and worldwide sea temperatures, 1901–85. *Nature* **320**, 602–607 (1986).
38. Rowell, D. P., Folland, C. K., Maskell, K., Owen, J. A. & Ward, M. N. Modelling the influence of global sea-surface temperatures on the variability and predictability of seasonal Sahel rainfall. *Geophysical Research Letters* **19**, 905–908 (1992).
39. Sutton, R. T. & Hodson, D. L. R. Atlantic Ocean forcing of North American and European summer climate. *Science* **309**, 115–118 (2005).
40. Folland, C. K., Colman, A. W., Rowell, D. P. & Davey, M. K. Predictability of northeast Brazil rainfall and real-time forecast skill, 1987–98. *Journal of Climate* **14**, 1937–1958 (2001).
41. Fensterer, C. *et al.* Cuban stalagmite suggests relationship between Caribbean precipitation and the Atlantic Multidecadal Oscillation during the past 1.3 ka. *Holocene* **22**, 1405–1412 (2012).
42. Enfield, D. B., Mestas-Núñez, A. M. & Trimble, P. J. The Atlantic multidecadal oscillation and its relation to rainfall and river flows in the continental US. *Geophysical Research Letters* **28**, 2077–2080 (2001).
43. McCabe, G. J., Palecki, M. A. & Betancourt, J. L. Pacific and Atlantic Ocean influences on multidecadal drought frequency in the United States. *Proceedings of the National Academy of Sciences* **101**, 4136–4141 (2004).
44. Alexander, M. A., Kilbourne, K. H. & Nye, J. A. Climate variability during warm and cold phases of the Atlantic Multidecadal Oscillation (AMO) 1871–2008. *Journal of Marine Systems* **133**, 14–26 (2014).
45. Moura, A. D. & Shukla, J. On the dynamics of droughts in northeast Brazil: Observations, theory and numerical experiments with a general circulation model. *Journal of Atmospheric Science* **38**, 2653–2675 (1981).
46. Goldenberg, S. B., Landsea, C. W., Mestas-Núñez, A. M. & Gray, W. M. The recent increase in Atlantic hurricane activity: Causes and implications. *Science* **293**, 474–479 (2001).
47. Magaña, V. O., Vázquez, J. L., Pérez, L. J. & Pérez, J. B. Impact of El Niño on precipitation in Mexico. *Geofísica Internacional* (2003), Vol. 42, Num. 3, pp. 313–330 **42** (2003).
48. Mendoza, B., Velasco, V. & Jáuregui, E. A Study of historical droughts in southeastern Mexico. *Journal of Climate* **19**, 2916–2934 (2006).
49. Karmalkar, A. V., Bradley, R. S. & Diaz, H. F. Climate change in Central America and México: regional climate model validation and climate change projections. *Climate Dynamics* **37**, 605–629 (2011).
50. Kennett, D. J. *et al.* Development and disintegration of Maya political systems in response to climate change. *Science* **338**, 788–791 (2012).
51. Gray, W. M. Atlantic seasonal hurricane frequency. Part I: El-Niño and 30-MB quasi-biennial oscillation influences. *Monthly Weather Review* **112**, 1649–1688 (1984).
52. Goldenberg, S. B. & Shapiro, L. J. Physical mechanisms for the Association of El Niño and West African rainfall with Atlantic Major Hurricane Activity. *Journal of Climate* **9**, 1169–1187 (1996).
53. Medina-Elizalde, M. *et al.* High resolution stalagmite climate record from the Yucatan Peninsula spanning the Maya terminal classic period. *Earth Planet Sc Lett* **298**, 255–262 (2010).
54. Baldini, L. M. *et al.* Persistent northward North Atlantic tropical cyclone track migration over the past five centuries. *Sci Rep-Uk* **6**, 37522 (2016).
55. Correa-Metrio, A. *et al.* Rapid climate change and no-analog vegetation in lowland Central America during the last 86,000 years. *Quaternary Sci Rev* **38**, 63–75 (2012).
56. Escobar, J. *et al.* A similar to 43-ka record of paleoenvironmental change in the Central American lowlands inferred from stable isotopes of lacustrine ostracods. *Quaternary Sci Rev* **37**, 92–104 (2012).
57. Krebs, U. & Timmermann, A. Tropical Air–Sea Interactions Accelerate the Recovery of the Atlantic Meridional Overturning Circulation after a Major Shutdown. *Journal of Climate* **20**, 4940–4956 (2007).
58. Yin, J., Schlesinger, M. E., Andronova, N. G., Malyshev, S. & Li, B. Is a shutdown of the thermohaline circulation irreversible? *Journal Geophysical Research* **111**, D12104 (2006).
59. Schmidt, M. W., Spero, H. J. & Lea, D. W. Links between salinity variation in the Caribbean and North Atlantic thermohaline circulation. *Nature* **428**, 160–163 (2004).
60. Lynch-Stieglitz, J. *et al.* Muted change in Atlantic overturning circulation over some glacial-aged Heinrich events. *Nature Geosci* **7**, 144–150 (2014).
61. Korty, R. L., Camargo, S. J. & Galeswsky, J. Tropical Cyclone Genesis Factors in Simulations of the Last Glacial Maximum. *Journal of Climate* **25**, 4348–4365 (2012).
62. Trenberth, K. E. & Fasullo, J. Energy budgets of Atlantic hurricanes and changes from 1970. *Geochem Geophys Geosy* **9** (2008).
63. Frappier, A. B. Masking of interannual climate proxy signals by residual tropical cyclone rainwater: Evidence and challenges for low-latitude speleothem paleoclimatology. *Geochem Geophys Geosy* **14**, 3632–3647 (2013).
64. Shen, C.-C. *et al.* Uranium and thorium isotopic and concentration measurements by magnetic sector inductively coupled plasma mass spectrometry. *Chem Geol* **185**, 165–178 (2002).
65. Lachniet, M. S. & Patterson, W. P. Oxygen isotope values of precipitation and surface waters in northern Central America (Belize and Guatemala) are dominated by temperature and amount effects. *Earth Planet Sc Lett* **284**, 435–446 (2009).
66. Adkins, J. F., McIntyre, K. & Schrag, D. P. The Salinity, Temperature, and  $\delta^{18}\text{O}$  of the Glacial Deep Ocean. *Science* **298**, 1769–1773 (2002).
67. Caley, T., Roche, D. M., Waelbroeck, C. & Michel, E. Oxygen stable isotopes during the Last Glacial Maximum climate: perspectives from data–model (iLOVECLIM) comparison. *Clim Past* **10**, 1939–1955 (2014).
68. Risi, C., Bony, S., Vimeux, F., Jouzel, J. & Edwards, R. L. Water-stable isotopes in the LMDZ4 general circulation model: Model evaluation for present-day and past climates and applications to climatic interpretations of tropical isotopic records. *Journal Geophysical Research* **115**, D12118 (2010).
69. Kim, S. T. & O’Neil, J. R. Equilibrium and nonequilibrium oxygen isotope effects in synthetic carbonates. *Geochim Cosmochim Acta* **61**, 3461–3475 (1997).
70. Rühlemann, C., Mulitza, S., Müller, P. J., Wefer, G. & Zahn, R. Warming of the tropical Atlantic Ocean and slowdown of thermohaline circulation during the last deglaciation. *Nature* **402**, 511–513 (1999).
71. Martrat, B. *et al.* Four Climate Cycles of Recurring Deep and Surface Water Destabilizations on the Iberian Margin. *Science* **317**, 502–507 (2007).
72. R Core Team (2013). R: A language and environment for statistical computing. R Foundation for Statistical Computing, Vienna, Austria. <http://www.R-project.org>.
73. Liu, Y., San Liang, X. & Weisberg, R. H. Rectification of the bias in the wavelet power spectrum. *Journal of Atmospheric and Oceanic Technology* **24**, 2093–2102 (2007).
74. Torrence, C. & Compo, G. P. A practical guide to wavelet analysis. *Bulletin of the American Meteorological Society* **79**, 61–78 (1998).

## Acknowledgements

We thank the Río Secreto Natural Reserve Board of Trustee and especially Mr. Otto Von Bertrab Schott for his support to our research. Special thanks to Tania Ramirez Rio Secreto's Director of Operations and the team of guides Rodrigo Pimienta, Rafael García and Victor Rodas for their enthusiasm, guidance and help in supporting our cave monitoring, field logistics, and speleothem collection. We thank Gabriela Serrato Marks (PhD student MIT) for running the COPRA analysis. We also thank Ing. Juan Pool, General Director of "Natural Stones Dealer", for generously helping us cut the Itzamna speleothem using his facilities and personnel. U-Th dating was supported by grants of Taiwan ROC Ministry of Science and Technology (MOST) (104-2119-M-002-003, 105-2119-M-002-001 to C.-C.S.) and National Taiwan University (105R7625) to C.-C.S. Fieldwork and isotopic analyses were supported by National Science Foundation grants # AGS-1502836 (M. Medina-Elizalde) and AGS-1502877 (S. Burns). J.M.P.M. was funded by a Basque Government post-doctoral fellowship. GPCC Precipitation data provided by the NOAA/OAR/ESRL PSD, Boulder, Colorado, USA, from their Web site at <http://www.esrl.noaa.gov/psd/>.

## Author Contributions

M.M.E. designed the project, prepared and wrote the manuscript, S.B. produced the stable isotope data, J.M.P.M. carried out the statistical and spectral analyses, F.L.H. produced the cave environmental monitoring data including drip, groundwater and meteoric water stable isotope data, R.B. contributed with data assimilation and evaluation of results, H.C.W. and C.C.S. carried out the uranium/thorium dating. All authors discussed the results and implications commented on the manuscript at all stages.

## Additional Information

**Supplementary information** accompanies this paper at doi:[10.1038/s41598-017-11742-8](https://doi.org/10.1038/s41598-017-11742-8)

**Competing Interests:** The authors declare that they have no competing interests.

**Publisher's note:** Springer Nature remains neutral with regard to jurisdictional claims in published maps and institutional affiliations.



**Open Access** This article is licensed under a Creative Commons Attribution 4.0 International License, which permits use, sharing, adaptation, distribution and reproduction in any medium or format, as long as you give appropriate credit to the original author(s) and the source, provide a link to the Creative Commons license, and indicate if changes were made. The images or other third party material in this article are included in the article's Creative Commons license, unless indicated otherwise in a credit line to the material. If material is not included in the article's Creative Commons license and your intended use is not permitted by statutory regulation or exceeds the permitted use, you will need to obtain permission directly from the copyright holder. To view a copy of this license, visit <http://creativecommons.org/licenses/by/4.0/>.

© The Author(s) 2017